

MICROSCOPIC CALCULATION OF FUSION; LIGHT TO HEAVY SYSTEMS

A. S. UMAR* and V. E. OBERACKER

*Physics and Astronomy, Vanderbilt University,
Nashville, TN 37235, USA*

**E-mail: umar@compsci.cas.vanderbilt.edu*

J.A. MARUHN

*Institut für Theoretische Physik, Goethe-Universität,
D-60438 Frankfurt am Main, Germany*

R. KESER

*RTE University, Science and Arts Faculty, Department of Physics, 53100,
Rize, TURKEY*

The density-constrained time-dependent Hartree-Fock (DC-TDHF) theory is a fully microscopic approach for calculating heavy-ion interaction potentials and fusion cross sections below and above the fusion barrier. We discuss recent applications of DC-TDHF method to fusion of light and heavy neutron-rich systems.

Keywords: Time-Dependent Hartree-Fock, Heavy-Ion Fusion, DC-TDHF.

1. Introduction

The investigation of internuclear potentials for heavy-ion collisions is of fundamental importance for the study of fusion reactions as well as for the formation of superheavy elements and nuclei far from stability. Recently, we have developed a new method to extract ion-ion interaction potentials directly from the time-dependent Hartree-Fock (TDHF) time-evolution of the nuclear system.¹ In the density-constrained TDHF (DC-TDHF) approach the TDHF time-evolution takes place with no restrictions. At certain times during the evolution the instantaneous density is used to perform a static Hartree-Fock minimization while holding the neutron and proton densities constrained to be the corresponding instantaneous TDHF densities. In essence, this provides us with the TDHF dynamical path in relation to the

multi-dimensional static energy surface of the combined nuclear system. In this approach there is no need to introduce constraining operators which assume that the collective motion is confined to the constrained phase space. In short, we have a self-organizing system which selects its evolutionary path by itself following the microscopic dynamics. Some of the effects naturally included in the DC-TDHF calculations are: neck formation, mass exchange, internal excitations, deformation effects to all order, as well as the effect of nuclear alignment for deformed systems. The DC-TDHF theory provides a comprehensive approach to calculating fusion barriers in the mean-field limit. The theory has been applied to calculate fusion cross-sections for $^{64}\text{Ni}+^{132}\text{Sn}$, $^{64}\text{Ni}+^{64}\text{Ni}$, $^{16}\text{O}+^{208}\text{Pb}$, $^{70}\text{Zn}+^{208}\text{Pb}$, $^{48}\text{Ca}+^{238}\text{U}$, and $^{132,124}\text{Sn}+^{96}\text{Zr}$ systems.²⁻⁸ In this paper we will outline the DC-TDHF method and give new examples of its application to the calculation of fusion cross-sections for various systems.

2. Density-Constrained TDHF Method

The concept of using density as a constraint for calculating collective states from TDHF time-evolution was first introduced in Ref. 10, and used in calculating collective energy surfaces in connection with nuclear molecular resonances in Ref. 9.

In this approach we assume that a collective state is characterized only by density ρ , and current \mathbf{j} . This state can be constructed by solving the static Hartree-Fock equations

$$\langle \Phi_{\rho,\mathbf{j}} | a_h^\dagger a_p \hat{H} | \Phi_{\rho,\mathbf{j}} \rangle = 0, \quad (1)$$

subject to constraints on density and current

$$\begin{aligned} \langle \Phi_{\rho,\mathbf{j}} | \hat{\rho}(\mathbf{r}) | \Phi_{\rho,\mathbf{j}} \rangle &= \rho(\mathbf{r}, t) \\ \langle \Phi_{\rho,\mathbf{j}} | \hat{\mathbf{j}}(\mathbf{r}) | \Phi_{\rho,\mathbf{j}} \rangle &= \mathbf{j}(\mathbf{r}, t). \end{aligned}$$

Choosing $\rho(\mathbf{r}, t)$ and $\mathbf{j}(\mathbf{r}, t)$ to be the instantaneous TDHF density and current results in the lowest energy collective state corresponding to the instantaneous TDHF state $|\Phi(t)\rangle$, with the corresponding energy

$$E_{coll}(\rho(t), \mathbf{j}(t)) = \langle \Phi_{\rho,\mathbf{j}} | \hat{H} | \Phi_{\rho,\mathbf{j}} \rangle. \quad (2)$$

This collective energy differs from the conserved TDHF energy only by the amount of internal excitation present in the TDHF state, namely

$$E^*(t) = E_{TDHF} - E_{coll}(t). \quad (3)$$

However, in practical calculations the constraint on the current is difficult to implement but we can define instead a static adiabatic collective state $|\Phi_\rho\rangle$ subject to the constraints

$$\begin{aligned}\langle \Phi_\rho | \hat{\rho}(\mathbf{r}) | \Phi_\rho \rangle &= \rho(\mathbf{r}, t) \\ \langle \Phi_\rho | \hat{j}(\mathbf{r}) | \Phi_\rho \rangle &= 0.\end{aligned}$$

In terms of this state one can write the collective energy as

$$E_{coll} = E_{kin}(\rho(t), \mathbf{j}(t)) + E_{DC}(\rho(\mathbf{r}, t)), \quad (4)$$

where the density-constrained energy E_{DC} , and the collective kinetic energy E_{kin} are defined as

$$\begin{aligned}E_{DC} &= \langle \Phi_\rho | \hat{H} | \Phi_\rho \rangle \\ E_{kin} &\approx \frac{m}{2} \sum_q \int d^3r \mathbf{j}_q^2(t) / \rho_q(t),\end{aligned}$$

where the index q is the isospin index for neutrons and protons ($q = n, p$). From Eq. 4 it is clear that the density-constrained energy E_{DC} plays the role of a collective potential. In fact this is exactly the case except for the fact that it contains the binding energies of the two colliding nuclei. One can thus define the ion-ion potential as¹

$$V = E_{DC}(\rho(\mathbf{r}, t)) - E_{A_1} - E_{A_2}, \quad (5)$$

where E_{A_1} and E_{A_2} are the binding energies of two nuclei obtained from a static Hartree-Fock calculation with the same effective interaction. For describing a collision of two nuclei one can label the above potential with ion-ion separation distance $R(t)$ obtained during the TDHF time-evolution. This ion-ion potential $V(R)$ is asymptotically correct since at large initial separations it exactly reproduces $V_{Coulomb}(R_{max})$. In addition to the ion-ion potential it is also possible to obtain coordinate dependent mass parameters. One can compute the ‘‘effective mass’’ $M(R)$ using the conservation of energy

$$M(R) = \frac{2[E_{c.m.} - V(R)]}{\dot{R}^2}, \quad (6)$$

where the collective velocity \dot{R} is directly obtained from the TDHF evolution and the potential $V(R)$ from the density constraint calculations.

3. Results

In this Section we give some recent examples of DC-TDHF calculations of heavy-ion potentials and cross-sections. Recently, we have studied the fusion of very neutron rich light nuclei that may be important to determine the composition and heating of the crust of accreting neutron stars.¹¹ The main focus was the O+O and C+O systems. For the $^{16}\text{O}+^{16}\text{O}$ system we have shown excellent agreement between our calculations and the low energy data from Refs.^{12,13} We have also extended this work to higher energies to see how our results compare with the available data. The reactions of light systems at high energies (2 – 3 times the barrier height) is complicated both experimentally and theoretically due to the presence of many breakup channels and excitations. All the data we could find date back to late 1970's.^{14–16} Experimental findings differ considerably in this energy regime as can be seen from Fig. 1. Recent analysis of the $^{16}\text{O}+^{16}\text{O}$ system by H. Esbensen¹⁷ primarily uses the data of Tserruya *et al.*¹⁵ We expect the TDHF results to yield a higher fusion cross-section since many of the breakup channels are not naturally available in TDHF. However, a close investigation of the TDHF dynamics and the microscopically calculated excitation energy clearly indicate that a significant portion of the collective kinetic energy is not equilibrated. It may be plausible to consider

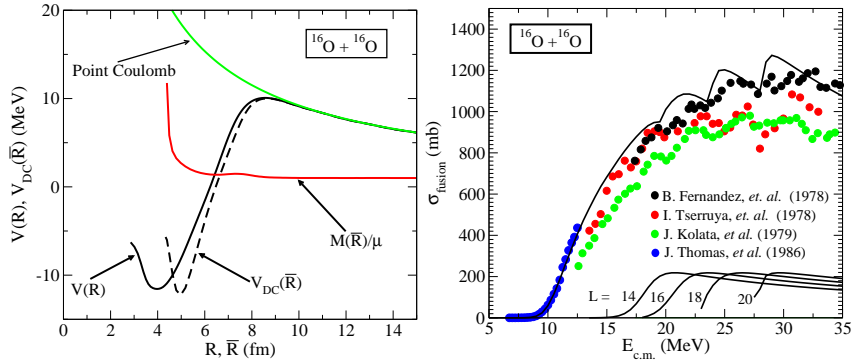


Fig. 1. (a) Ion-Ion potential and effective mass for $^{16}\text{O}+^{16}\text{O}$. (b) Corresponding fusion cross-sections.

the direct influence of the excitation energy, $E^*(R)$, on the fusion barriers by making an analogy with the coupled-channel approach and construct a new potential $V^*(R) = V(R) + E^*(R)$, which has all the excitations added to the ion-ion potential $V(R)$ that should be calculated at higher energies to

minimize the nuclear rearrangements (frozen-density limit). The resulting potentials somewhat resemble the repulsive-core coupled-channel potentials of Ref.¹⁸ This approach does lead to improvements in cases where most of the excitation energy is in the form of collective excitations rather than irreversible stochastic dissipation (true especially for lighter systems). The viability of this approach requires further examination and will be studied in the future. It is interesting to note that the gross oscillations in the cross-section at higher energies are correctly reproduced in our calculations. This is simply due to opening of new L -channels as we increase the collision energy. Individual contributions to the cross-section from higher L values are also shown on the lower part of the plot.

In Fig. 2a we show the DC-TDHF potential barriers for the C+O system. The higher barrier corresponds to the $^{12}\text{C} + ^{16}\text{O}$ system and has a peak energy of 7.77 MeV. The barrier for the $^{12}\text{C} + ^{24}\text{O}$ system occurs at a slightly larger R value with a barrier peak of 6.64 MeV. Figure 2b shows the corresponding cross sections for the two reactions. Also shown are the experimental data from Refs. 19–21. The DC-TDHF potential reproduces the experimental cross-sections quite well for the $^{12}\text{C} + ^{16}\text{O}$ system, and the cross section for the neutron rich $^{12}\text{C} + ^{24}\text{O}$ is predicted to be larger than that for $^{12}\text{C} + ^{16}\text{O}$.

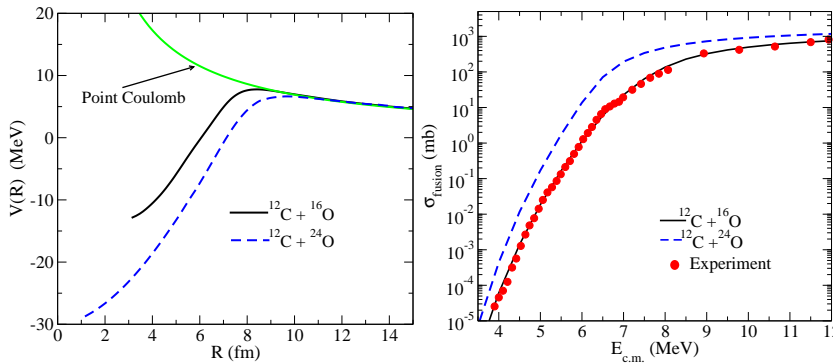


Fig. 2. (a) Ion-Ion potential for various isotopes of the C+O system. (b) Corresponding cross-sections.

Figures 3a and 3b show the corresponding potentials and cross-sections for the Ca+Ca system,²² which was the subject of recent experimental studies.²³ The observed trend for sub-barrier energies is typical for DC-TDHF calculations when the underlying microscopic interaction gives a good rep-

resentation of the participating nuclei. Namely, the potential barrier corresponding to the lowest collision energy gives the best fit to the sub-barrier cross-sections since this is the one that allows for more rearrangements to take place and grows the inner part of the barrier. Considering the fact that historically the low-energy sub-barrier cross-sections of the $^{40}\text{Ca}+^{48}\text{Ca}$ system have been the ones not reproduced well by the standard models, the DC-TDHF results are quite satisfactory, indicating that the dynamical evolution of the nuclear density in TDHF gives a good overall description of the collision process. The shift of the cross-section curve with increasing collision energy is typical. In principle one could perform a DC-TDHF calculation at each energy above the barrier and use that cross-section for that energy. However, this would make the computations extremely time consuming and may not provide much more insight. The trend at higher energies for the $^{40}\text{Ca}+^{48}\text{Ca}$ system is atypical. The calculated cross-sections are larger than the experimental ones by about a factor of two. Such lowering of fusion cross-sections with increasing collision energy is commonly seen in lighter systems where various inelastic channels, clustering, and molecular formations are believed to be the contributing factors.

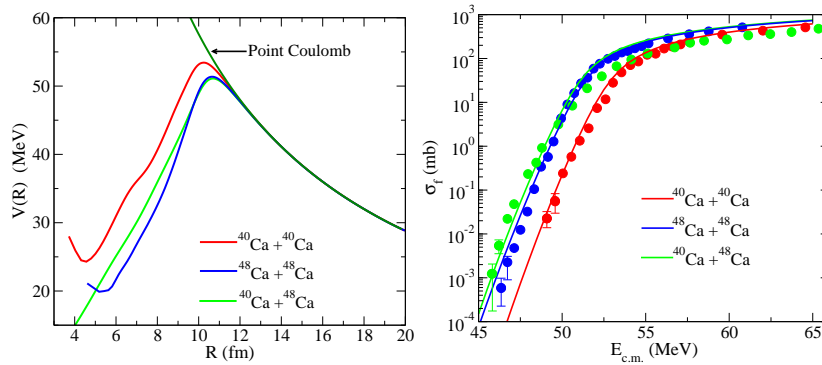


Fig. 3. (a) Ion-Ion potential for various isotopes of the Ca+Ca system. (b) Corresponding cross-sections.

Recently, we have also provided extensive studies of the neutron-rich systems $^{132}\text{Sn}+^{40}\text{Ca}$ and $^{132}\text{Sn}+^{48}\text{Ca}$.²⁴ Such systems typically have energy dependent potentials. Figure 4a shows our DC-TDHF calculations compared with the experimental data²⁵ for the $^{132}\text{Sn}+^{48}\text{Ca}$ system. If one compares the measured fusion cross sections for both systems at low energies, one finds the surprising result that fusion of ^{132}Sn with ^{40}Ca yields

a larger cross section than with ^{48}Ca . For example, at $E_{\text{c.m.}} = 110$ MeV we find an experimental cross section of ≈ 6 mb for $^{132}\text{Sn}+^{40}\text{Ca}$ as compared to 0.8 mb for the more neutron-rich system $^{132}\text{Sn}+^{48}\text{Ca}$. This behavior can be understood by examining the DC-TDHF heavy-ion potentials, in Fig. 4b, which have been calculated at the same center-of-mass energy $E_{\text{TDHF}} = 120$ MeV. We observe that while the barrier heights and positions for both systems are approximately the same, the *width* of the DC-TDHF potential barrier for $^{132}\text{Sn}+^{40}\text{Ca}$ is substantially smaller than for $^{132}\text{Sn}+^{48}\text{Ca}$, resulting in enhanced sub-barrier fusion at low energy.

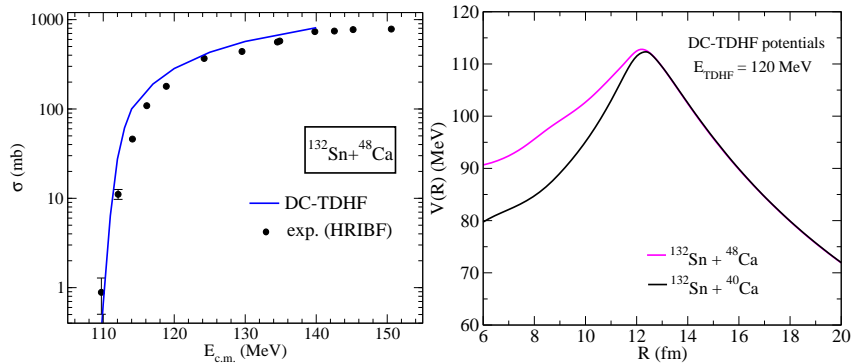


Fig. 4. (a) DC-TDHF results for $^{132}\text{Sn}+^{48}\text{Ca}$ system compared to data. (b) Ion-ion potentials for the $^{132}\text{Sn}+^{40,48}\text{Ca}$ systems.

4. Conclusions

We have provided some of the recent result for fusion cross-sections obtained by the microscopic DC-TDHF method. DC-TDHF method is shown to be a powerful method for such calculations and can be readily generalized to other dynamical microscopic theories. Considering the fact that the fitting of the Skyrme force parameters contains no dynamical information the result are very promising.

Acknowledgments

This work has been supported by the U.S. Department of Energy under grant No. DE-FG02-96ER40975 with Vanderbilt University.

References

1. A. S. Umar and V. E. Oberacker *Phys. Rev. C* **74** 021601(R) (2006).
2. A. S. Umar and V. E. Oberacker *Phys. Rev. C* **74** 024606 (2006).
3. A. S. Umar and V. E. Oberacker *Phys. Rev. C* **74** 061601(R) (2006).
4. A. S. Umar and V. E. Oberacker *Phys. Rev. C* **76** 014614 (2007).
5. A. S. Umar and V. E. Oberacker *Phys. Rev. C* **77** 064605 (2008).
6. A. S. Umar and V. E. Oberacker *Eur. Phys. J. A* **39**, 243 (2009).
7. A. S. Umar , V. E. Oberacker , J. A. Maruhn and P.-G. Reinhard, *Phys. Rev. C* **81**, 064607 (2010).
8. V. E. Oberacker,A. S. Umar, J. A. Maruhn, and P.-G. Reinhard, *Phys. Rev. C* **82**, 034603 (2010).
9. A. S. Umar, M. R. Strayer, R. Y. Cusson, P. -G. Reinhard, and D. A. Bromley, *Phys. Rev. C* **32**, 172 (1985).
10. R. Y. Cusson, P.-G. Reinhard, M. R. Strayer, J. A. Maruhn, and W. Greiner, *Z. Phys. A* **320**, 475 (1985).
11. A. S. Umar, V. E. Oberacker, and C.J. Horowitz, *Phys. Rev. C* **85**, 055801 (2012).
12. J. Thomas, Y. T. Chen, S. Hinds, K. Langanke, D. Meredith, M. Olson, and C. A. Barnes, *Phys. Rev. C* **31**, 1980 (1985).
13. J. Thomas, Y. T. Chen, S. Hinds, D. Meredith, and M. Olson, *Phys. Rev. C* **33**, 1679 (1986).
14. B. Fernandez, C. Gaarde, J. S. Larsen, S. Pontoppidan, and F. Videbaek, *Nucl. Phys.* **A306**, 259 (1978).
15. I. Tserruya, Y. Risen, D. Pelte, A. Gavron, H. Oeschler, D. Berndt, and H.L Harney, *Phys. Rev. C* **18**, 1688 (1978).
16. J. J. Kolata, R. M. Freeman, F. Haas, B. Heusch, and A. Gallmann, *Phys. Rev. C* **19**, 2237 (1979).
17. H. Esbensen, *Phys. Rev. C* **77**, 054608 (2008).
18. H. Esbensen *et al.*, *Phys. Rev. C* **82**, 054621 (2010).
19. C. L. Jiang, K. E. Rehm, B. B. Back, and R. V. F. Janssens, *Phys. Rev. C* **75**, 015803 (2007).
20. H. W. Becker *et al.*, *Z. Phys.* **A303**, 305 (1981).
21. L. R. Gasques *et al.*, *Phys. Rev. C* **72**, 025806 (2005).
22. R. Keser, A. S. Umar, and V. E. Oberacker, *Phys. Rev. C* **85**, 044606 (2012).
23. G. Montagnoli *et al.*, *Phys. Rev. C* **85**, 024607 (2012).
24. V.E. Oberacker, A.S. Umar, J.A. Maruhn, and P.-G. Reinhard, *Phys. Rev. C* **85**, 034609 (2012).
25. J. J. Kolata, *et al.*, *Phys. Rev. C* **85**, 054603 (2012).